Journal of Catalysis 280 (2011) 230–238

Contents lists available at ScienceDirect

Journal of Catalysis

journal homepage: www.elsevier.com/locate/jcat

Analysis of the promotion of $CoMoP/Al_2O_3$ HDS catalysts prepared from a reduced H–P–Mo heteropolyacid Co salt

Adolfo Romero-Galarza, Aída Gutiérrez-Alejandre, Jorge Ramírez *

UNICAT, Depto. de Ingeniería Química, Fac. de Química, Universidad Nacional Autónoma de México, Cd. Universitaria, México, DF 04510, Mexico

ARTICLE INFO

Article history:
Received 1 February 2011
Revised 22 March 2011
Accepted 23 March 2011
Available online 6 May 2011

Keywords:
Promotion
HDS
4,6-DMDBT
$Co_{7/2}PMo_{12}O_{40}$
Reduced heteropolyacid
CO adsorption

ABSTRACT

HDS activity of 4,6-DMDBT for calcined and non-calcined $CoMoP/Al_2O_3$ catalysts prepared with $Co_{7/2}PMo_{12}O_{40}$ was compared with that of a catalyst prepared conventionally by coimpregnation with a solution containing ammonium heptamolybdate, cobalt nitrate, and phosphoric acid. The extent of promotion for each method of preparation was quantitatively determined by CO adsorption, and the intrinsic activity of the different coordinatively unsaturated Mo sites in the catalyst was evaluated. The use of $Co_{7/2}PMo_{12}O_{40}$ as catalyst precursor leads to higher HDS activity than the catalyst prepared by coimpregnation. The high activity of the former catalyst was related to a higher number of Co-promoted molybdenum sites. The number of Co-promoted sites depends on the pretreatment before sulfidation, particularly calcination. Highest activity is obtained by avoiding calcination, and the activity decreases with the calcination temperature. Two different types of promoted CoMoS sites with different HDS intrinsic activities seem to coexist in the sulfided catalyst.

1. Introduction

The need to process heavier petroleum feeds caused by the diminishing trend of light oil supplies, and the more strict environmental regulations on the sulfur content in transport fuels are among the major driving forces to develop more active hydrodesulfurization catalysts, capable of eliminating the most refractory sulfur-containing molecules such as the beta-substituted dibenzothiophenes (i.e., 4,6-dimethyldibenzothiophene).

For the hydrodesulfurization of petroleum fractions, Mo or W sulfide catalysts promoted by Co or Ni and supported over γ-alumina are used. It is believed that the sulfur vacancies at the edges of the MoS_2 crystallites are very important to catalytic activity [1–7] and that the catalytic properties of these sites are strongly enhanced by the close presence of a promoter atom (Co or Ni) in the so-called Co(Ni)–Mo–S structures [8,9,2,10–16]. It has been reported that complete sulfidation of the molybdenum phase leads to the so-called type II Co(Ni)–Mo–S sites, that are more active than the partially sulfided type I sites, which strongly interact with the catalyst support via Mo–O bridges [10,12,17]. So, the production of highly active hydrodesulfurization catalysts depends to a greater extent on the level of promotion reached during the catalyst preparation. To increase the number of promoted Co(Ni)–Mo–S sites, it is desirable for the Co(Ni) and Mo atoms to be as close as possible during the activation (sulfidation) of the catalyst. Therefore, an interesting alternative is the use of a single precursor salt that already contains in its structure both atoms, Mo and Co, in the desired ratio, instead of using two precursor salts, one of the Mo and one of the Co, as in the conventional catalyst preparation procedure.

Several investigators have previously suggested the use of Mo or W heteropolyacids with Keggin structure [18,19] as precursors for the preparation of HDS catalysts. In general, the preparation utilizes a solution of a commercial heteropolyacid such as $H_3PMo_{12}O_{40}$ to which Co or Ni are incorporated in the form of nitrates in the necessary amount to reach a Co(Ni)/Co(Ni)+Mo ratio around 0.33, which is the one reported as optimum for conventionally prepared HDS catalysts [20]. However, this method of preparation leads to an heteropolyacid salt, $Co_{3/2}PMo_{12}O_{40}$, with a ratio of Co/Co + Mo = 0.11, plus an excess of Co or Ni nitrate, which will have the disadvantages of the traditional method of preparation, i.e., the possibility of forming segregated Co species during the calcination or sulfidation of the catalyst and a greater probability of interaction of the Co-promoter with the alumina support leading to inactive cobalt aluminate species. Alumina-supported catalysts of this type have been evaluated in the HDS of thiophene [21–24], others supported on mesoporous silica (HMS) have been tested in the HDS of benzothiophene [19,25], and only a few in the HDS of refractory compounds such as 4,6-DMDBT [26]. The results showed that catalysts prepared from heteropolyacids are more active in HDS of thiophene and 4,6-DMDBT than catalysts prepared from conventional precursors.

* Corresponding author.
E-mail address: jrs@servidor.unam.mx (J. Ramírez).

0021-9517/$ - see front matter © 2011 Elsevier Inc. All rights reserved.
doi:10.1016/j.jcat.2011.03.021

To increase the promotion Co/Co + Mo in the Keggin structure, Grivobal et al. [21] proposed to partially reduce the Keggin anion $[PMo_{12}O_{40}]^{-3}$ to $[PMo_{12}O_{40}]^{-7}$ and in this way increase the exchange sites in the anion and achieve a Co/Co + Mo ratio of 0.23 in the final Co salt. The studies carried out with this reduced salt in the HDS of thiophene showed that the activity of the catalyst prepared with the salt of the reduced heteropolyacid were 32% more active than its conventional counterpart. The results also showed that the activity of the catalyst calcined at 400 °C was greater than the uncalcined one. This result is surprising since one would expect that the uncalcined catalyst where both Mo and Co are in the same structural entity will lead, during the catalyst activation (sulfidation), to a greater number of promoted Co–Mo–S sites. It appears necessary to carry out a detailed study of the amount of promoted and unpromoted Mo sites formed in the sulfided catalysts to establish beyond doubt the advantage of using Co salts of the reduced heteropolyacid to prepare the catalyst.

To our knowledge, no studies have been reported on the hydrodesulfurization of refractory compounds such as 4,6-DMDBT using Co salts of reduced Keggin anions such as $[PMo_{12}O_{40}]^{-7}$. Additionally, although it is assumed that the use of heteropolyacid salts might lead to a better promotion, a quantitative evaluation of the number of promoted and unpromoted sites obtained by using salts of reduced heteropolyacids is absent in the open literature. Therefore, in the present work, $CoMoP/Al_2O_3$ catalysts prepared from a reduced Co Keggin salt ($Co_{7/2}PMo_{12}O_{40}$) were tested in the HDS of 4,6-DMDBT. The state and transformations of the precursor salt before sulfidation were characterized by nitrogen physisorption, Raman spectroscopy, and X-ray diffraction. After sulfidation, the catalysts were characterized by high-resolution transmission electron microscopy (HRTEM), and CO adsorption analyzed by FTIR. This last study allowed us to relate the observed changes in catalytic activity with the amount of promoted and unpromoted Mo sites present in the sulfided catalysts, for different catalyst preparation procedures.

2. Experimental

2.1. Precursor salt and catalysts preparation

The reduced heteropolyacid $H_7PMo_{12}O_{40}$, was prepared following the procedure described by Griboval et al. [21]. The reduced heteropolyacid was prepared in an inert atmosphere by reacting sodium molybdate (99%, FLUKA), phosphoric acid (85.4%, JT Baker), and $MoOCl_5^{2-}$ (98%, Aldrich), the latter obtained by hydrolysis in a 3 M solution of $MoCl_5$ in HCl (37%, Aldrich), according to the following equation [21]:

$$H_3PO_4 + 8MoO_4^{2-} + 4MoOCl_5^{2-} + 4H^+ \rightarrow H_7PMo_{12}O_{40} + 20Cl^-$$

$Co_{7/2}PMo_{12}O_{40}$, was obtained by cationic exchange of cobalt using cobalt carbonate (96% JT Baker), with the protonic sites of $H_7PMo_{12}O_{40}$, according to the method described in the study by Grivobal et al. [21,27].

$CoMoP/Al_2O_3$ catalysts with 2.8 Mo atoms/nm^2 and a Co/Co + Mo ratio of 0.23, which correspond to 12.2 wt.% MoO_3, 1.85 wt.% CoO and 0.6 wt.% P_2O_5, were prepared. The alumina support was impregnated with an aqueous solution of $Co_{7/2}PMo_{12}O_{40}$ using the pore volume impregnation method. After, the catalyst was aged for 2 h at room temperature, dried at 100 °C for 24 h at ambient conditions, and calcined at 350 or 400 °C for 4 h using a heating rate of 1 °C/min under nitrogen flow (20 ml/min). Catalysts are denoted CoMoP/Al D, CoMoP/Al 350, and CoMoP/Al 400, where D = dry catalyst, and 350 and 400 correspond to the calcination temperatures used. For reference, a catalyst with the same composition was prepared impregnating the alumina support with aqueous solutions of ammonium heptamolybdate (AHM), (97% Aldrich), cobalt nitrate (98% Aldrich), and phosphoric acid (85.4%, JT Baker). This catalyst, named CoAHM/Al 400, was dried at 100 °C for 24 h and calcined in air at 400 °C for 4 h. Additionally, two unpromoted catalysts, MoP/Al D and MoP/Al 400, were prepared using a similar procedure as for CoMoP.

2.2. Characterization of $Co_{7/2}PMo_{12}O_{40}$

The spectroscopic analysis of $Co_{7/2}PMo_{12}O_{40}$ was performed in a NICOLET mod. Magna 760 FTIR with 100 scans per spectrum and a resolution of 4 cm^{-1}. The elemental analysis of the precursor salt ($Co_{7/2}PMo_{12}O_{40}$) was obtained with a OXFORD, ISIS model microanalysis coupled to a JEOL-5900-LV SEM microscope. At the conditions used, 20 kV, the depth of analysis was 2 μm. X-ray diffraction analysis between $3° \leqslant 2\theta \leqslant 90°$ was performed with a Phillips PW 1050/25 diffractometer using Cu Kα radiation (λ = 1.5418 Å).

2.3. Characterization of oxide catalysts

The textural properties (surface area, pore diameter, and pore volume) of the catalysts were obtained using an automatic Micromeritics TriStar 3000 nitrogen physisorption apparatus. Prior to the measurements, all samples were outgassed at 270 °C for 3 h (Micromeritics Vac Prep 061). The Raman spectra of the samples were recorded at room temperature using a Nicolet 950 FT Raman equipped with an In Ga As detector and a He–Ne source laser.

2.4. Characterization of sulfided catalysts

HRTEM micrographs of the sulfided catalysts were obtained with a JEOL 2010 transmission electron microscope operating at 200 kV with 1.9 Å point to point resolution. The samples were dispersed by ultrasonication in heptanes for 20 min, and a drop of the supernatant liquid was placed on a holey carbon film supported on a copper grid. For the statistical analysis of the size and stacking distribution of MoS_2 crystallites, more than 300 crystallites were measured.

2.5. Infrared spectroscopy: CO adsorption

For CO adsorption experiments, self-supporting wafers of 6.7 mg/cm^2 of pure catalyst powder were made, placed in the IR cell, and then sulfided at the same conditions as used in the catalytic activity tests. Subsequently, the cell was outgassed in vacuum at 723 K for 2 h. CO adsorption at 100 K was performed by adding small pulses of CO up to a pressure of 1 Torr equilibrium. The spectra were taken with a Nicolet Magna 760 FTIR spectrophotometer with a resolution of 4 cm^{-1} and 100 scans per spectrum. The integrated molar extinction coefficients ε of CO adsorbed on the sulfided catalysts [28,29] were determined in the IR cell at liquid nitrogen temperature (100 K) by the introduction of very small doses of CO (0.005 Torr). The following values were used in this work: ε Mo (band at 2110 cm^{-1}) = 18 cm μmol^{-1}, ε CoMoS (band at 2070 cm^{-1}) = 28 cm μmol^{-1}.

2.6. Temperature Programmed Sulfidation (TPS)

Two hundred and fifty milligrams of catalyst was placed in a quartz reactor under a continuous flow of 19.6 mL/min of 5 vol.% of H_2S in H_2. The sample was heated at 10 °C/min from room temperature to 873 K and then maintained at this temperature for half an hour. The consumption of H_2S was followed with a Cary 50 UV–Vis spectrophotometer working with a fixed wavelength of 200 nm.

2.7. Catalytic evaluation

Prior to the catalytic test, the catalyst was activated ex situ in a continuous flow reactor using 20 mL/min of a H_2S (15 vol.%)/H_2 gas mixture at 673 K during 4 h. The reaction test was carried out in a batch Parr reactor operating at 593 K and 1200 psi, using 200 mg of catalyst in 40 mL of decane containing 1000 ppm of sulfur as 4,6-DMDBT. For calculation of the rate constants for 4,6-DMDBT disappearance, an irreversible pseudo-first-order reaction rate was considered, $r_{4,6} = k_{4,6}C_{4,6}^{\alpha}$ ($\alpha = 1.0$). The value of the rate constant was then obtained from the slope of the linear expression: $Ln(C_{4,6}°/C_{4,6}) = k_{4,6}t$, where t = reaction time.

The analysis of the reaction products was performed on a HP 6890 gas chromatograph equipped with a HP-1 column of 100 m length and 0.025 mm diameter and a flame ionization detector. Samples were taken each hour during 6 h.

3. Results and discussion

3.1. Characterization of $Co_{7/2}PMo_{12}O_{40}$

The FTIR spectrum of $H_7PMo_{12}O_{40}$ (Fig. 1) show bands at 1022, 965, a shoulder at 974, and 800 cm^{-1}, characteristic of the Keggin structure [21,30,31], assigned to νP—O (1022 cm^{-1}), νMo═O (965, 978 cm^{-1}), and νMo—O—Mo (800 cm^{-1}). In the cobalt salt, $Co_{7/2}PMo_{12}O_{40}$, the last three bands appear at similar wavenumber and the band at 1022 cm^{-1} appears shifted to 1065 cm^{-1}. These results confirm the presence of the reduced entity $Co_{7/2}PMo_{12}O_{40}$, as reported by Grivobal et al. [21].

The results from SEM-EDX in Table 1 indicate that the experimental Co/Co + Mo ratio as measured by SEM-EDX in the synthesized Keggin-reduced Co salt structure was 0.23, in good agreement with the stoichiometric value for $Co_{7/2}$ $PMo_{12}O_{40}$, indicating that the synthesis of the reduced salt was well achieved.

The stability of the Keggin salt at the different calcination temperatures used in this work can be followed by X-ray diffraction. However, due to the detection limits of the technique, to better observe the transformations of the Keggin salt with the calcination temperature, this study was carried out not with the supported catalyst, which contains about 12 wt.% of well-dispersed Keggin salt, but with the bulk heteropolyacid salt, $Co_{7/2}PMo_{12}O_{40}$. The results are shown in Fig. 2 where the bulk heteropolyacid precursor has also been included for reference.

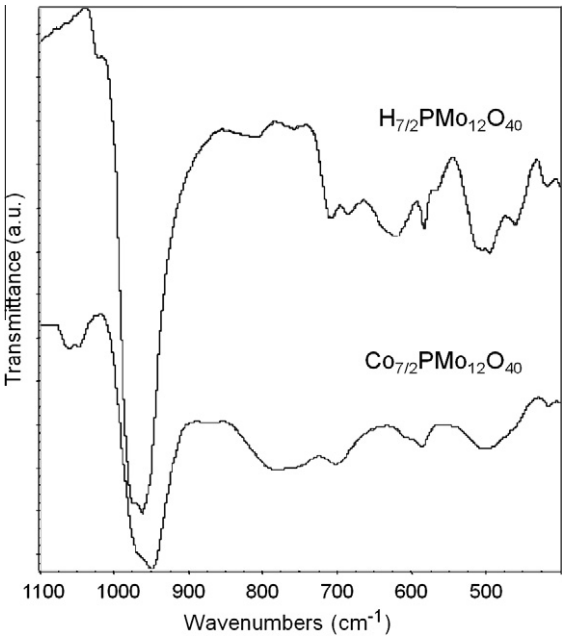

Fig. 1. FTIR spectra of the heteropolyacid and its Co salt.

Table 1
Elemental analysis of salt $Co_{7/2}PMo_{12}O_{40}$.

Element	Atomic %
O	57.1
P	2.1
Co	8.9
Mo	29.3
Co/(Co + Mo)	0.23

According to the reported literature data [21], the diffraction peaks in the 2θ region between 20° and 33° are characteristic of the oxygen lattice in the Keggin structure. The diffraction pattern of the uncalcined Co heteropolyacid salt, which presents an intense peak at $2\theta = 26.7°$ and two more at $2\theta = 30.6$ *y* 32.8°, shows some changes with respect to the heteropolyacid suggesting, as reported previously, that the introduction of cobalt induces a modification of the lattice parameters [21]. After calcination at 350 °C, the intensity of the peaks decreases and three new peaks appear at $2\theta = 25$, 27.4 *y* 27.8°, suggesting the partial decomposition of the cobalt salt. This can be due to the rearrangement of the crystalline lattice caused by the loss of crystallization water or to the formation of a lacunary structure (i.e., $Co_{7/2}PMo_{12-x}O_{40-y}$). Calcination at 400 °C causes the appearance of new peaks at $2\theta = 23.3°$ and 27.3° [31], assigned to α-MoO_3, indicating the decomposition of the cobalt salt at this calcination temperature.

The results indicate that the bulk Keggin Co salt is stable in nitrogen atmosphere below 350 °C and that above 400 °C it decomposes, most probably to the corresponding Co and Mo oxides. Several works dealing with the preparation of HDS catalysts from heteropolyacids have used a calcination temperature of 400 °C.

3.2. Characterization of catalysts before sulfidation

The textural properties of the alumina support and catalysts are presented in Table 2. Incorporation of the Keggin salt to the support causes a small decrease in the specific surface area, which is slightly enhanced with the calcination temperature. Impregnating the catalyst with AHM and cobalt nitrate gives similar decrease in surface area.

The pore size distribution plot (Fig. 3) shows smaller diameter pores for all the catalysts prepared with the Keggin salt respect to the one prepared with AHM. This can be due either to the

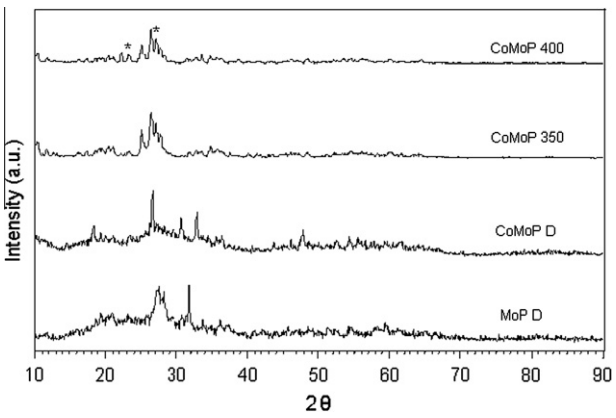

Fig. 2. X-ray diffractograms for $H_7PMo_{12}O_{40}$ (MoP), and bulk $Co_{7/2}PMo_{12}O_{40}$, dried (D) and calcined at 350 and 400 °C; ∗ α-MoO_3.

Table 2
Textural properties of support and catalysts.

Sample	Specific surface (m^2/g)	Average pore diameter (Å)	Average pore volume (cc/g)
Al_2O_3	206	93	0.56
CoMoP/Al D	183	83	0.43
CoMoP/Al 350	180	88	0.41
CoMoP/Al 400	174	91	0.43
CoAHM/Al 400	188	71	0.45

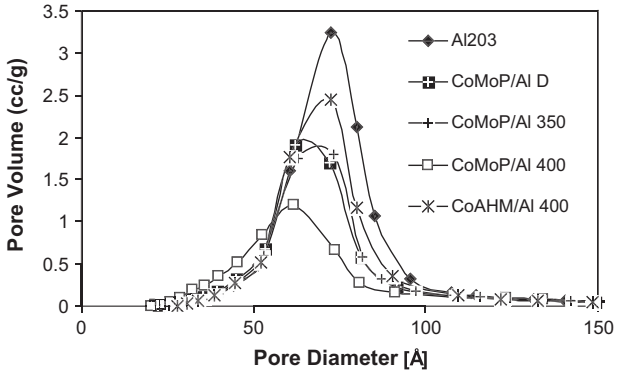

Fig. 3. Pore size distribution curves for the alumina support and catalysts.

bulkiness of the Keggin salt entity per mole of Mo compared with AHM or to a greater blockage of pores during the impregnation of the Keggin salt.

The diffractograms of CoMoP/Al D and CoMoP/Al 350 (Fig. 4) do not present the characteristic peaks associated with the Keggin salt in the region $2\theta = 20–33°$ [21], suggesting either good dispersion or decomposition of the Keggin unit. Calcination at 400 °C causes the appearance of a peak at $2\theta = 26°$, which could be associated with a distorted Keggin structure of a size detectable by the technique. The XRD pattern of the catalyst prepared with AHM and calcined at 400 °C presents small peaks at $2\theta = 27$ *y* 23 associated with the α-MoO_3 phase [31].

To enquire further on the evolution of the Keggin structure upon calcination, Raman experiments were carried out.

The Raman spectrum corresponding to the salt precursor (CoMoP) shows the main peaks assigned to the Keggin structure [21,27,31–33] localized at 985 cm^{-1} (ν_s Mo═O_T), 876 cm^{-1} (ν_{as} Mo—O_b—Mo), and 242 cm^{-1} (δ Mo—O_p). The band at 933 cm^{-1} (ν_{as} Mo═O_T), which cannot be assigned to MoO_3, could be

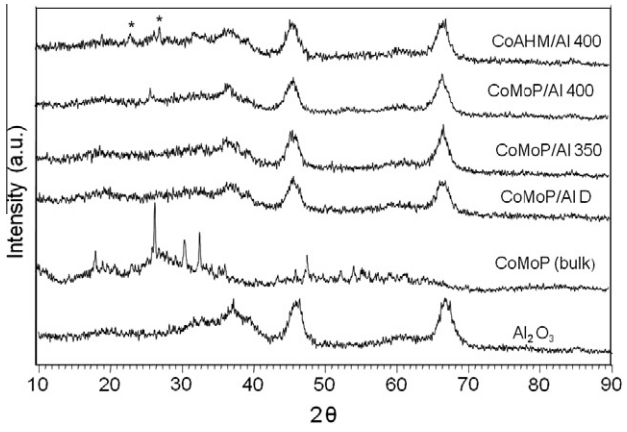

Fig. 4. X-ray diffractograms of $Co_{7/2}PMo_{12}O_{40}$, Al_2O_3, and catalysts; ∗ α-MoO_3.

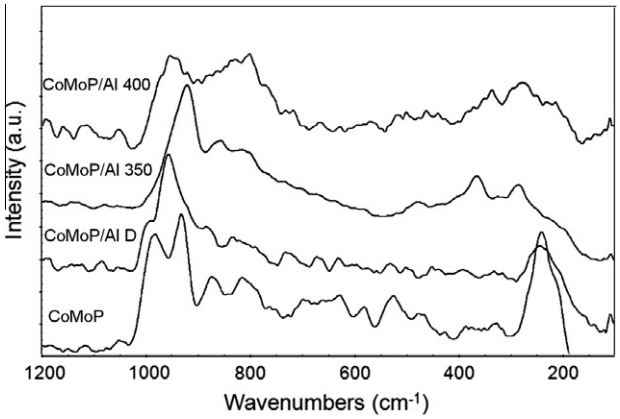

Fig. 5. Raman spectra of CoMoP/Al catalysts.

originated by a partial decomposition of the structure by the intensity of the laser beam [21] (see Fig. 5).

After impregnation of $Co_{7/2}PMo_{12}O_{40}$ to the alumina support, dried catalyst, there is a variation in the characteristic Raman peak intensities of the Keggin unit, being more significant for the peak at 242 cm^{-1}.

When the CoMoP/Al catalyst is calcined at 350 °C, the overall Raman spectrum changes disappearing almost the peak at 985 cm^{-1} (ν_s Mo═O_T) and that localized at 933 cm^{-1} (ν_{as} Mo—O_T) is shifted to 924 cm^{-1}, indicating a partially decomposition of the Keggin structure. The fact that the characteristic peak due to the vibration mode of the Mo—O_T bond is preserved, indicates that the Keggin units have not completely collapsed. At higher calcination temperature (400 °C), the absence of the peak at 985 cm^{-1} and the appearance of an intense peak with two maxima at ∼952 cm^{-1} and at ∼827 cm^{-1} suggest that at these temperatures, the heteropolycompound is transformed into polymolybdates [32–35,4,36] and MoO_3 crystals [32,33].

3.3. Characterization of sulfided catalysts

The performance of sulfide Co(Ni)Mo HDS catalysts depends, among other things, on the morphology and dispersion of the MoS_2 crystallites. The use of Co salts of heteropolyacids as precursors of the active CoMoS phase can change the degree of promotion and the dispersion of the supported active phases. The degree of dispersion will also be affected by the different treatments given to the catalyst before activation (i.e., drying and calcination conditions).

The morphology of the Mo sulfide supported phase for the different catalysts can be observed in Fig. 6. All catalysts present the typical MoS_2 slabs with different length and stacking with interplanar distance of 6.1 Å [37,38]. In general, all the catalysts present high dispersion with MoS_2 crystallites with one or two layers and lengths mostly in the range 20–50 Å.

To estimate the relative dispersion of the observable MoS_2 crystallites, a distribution of the length and stacking was built measuring more than 300 crystallites per sample. The results from this exercise are presented in Fig. 7. The dry and calcined catalysts prepared with $Co_{7/2}PMo_{12}O_{40}$ show the maximum population of MoS_2 crystallites with one layer and lengths between 21 and 40 Å. The catalyst prepared with AHM shows similar values for the stacking but larger lengths of the MoS_2 crystallites compared with the catalysts prepared with the heteropolyacid Co salt.

The distributions of length and stacking degree for the different catalysts are presented in Fig. 7; the average values of length and stacking of MoS_2 crystallites and the fraction of Mo atoms in edge

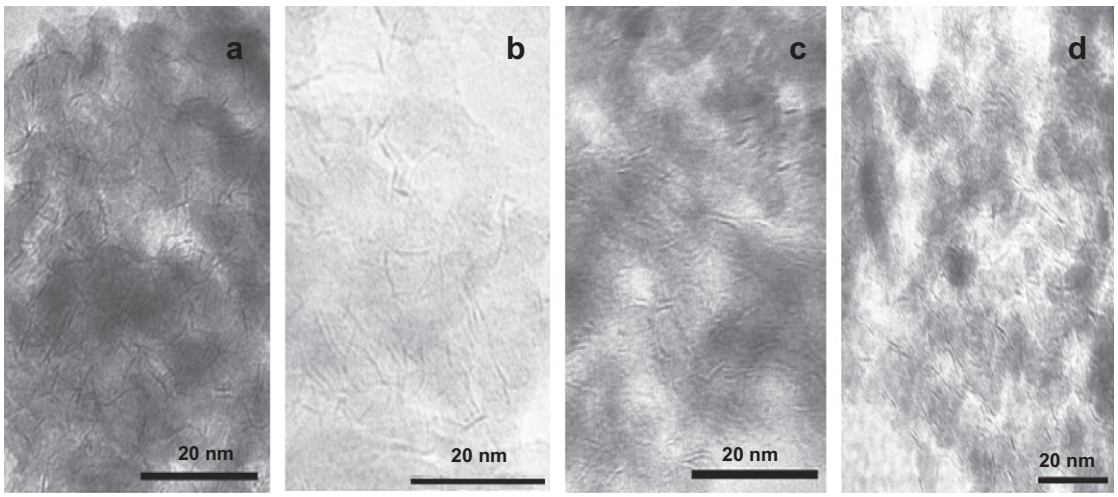

Fig. 6. HRTEM micrographs of sulfided catalysts, (a) CoMoP/Al D, (b) CoMoP/Al 350, (c) CoMoP/Al 400, (d) CoAHM/Al 400.

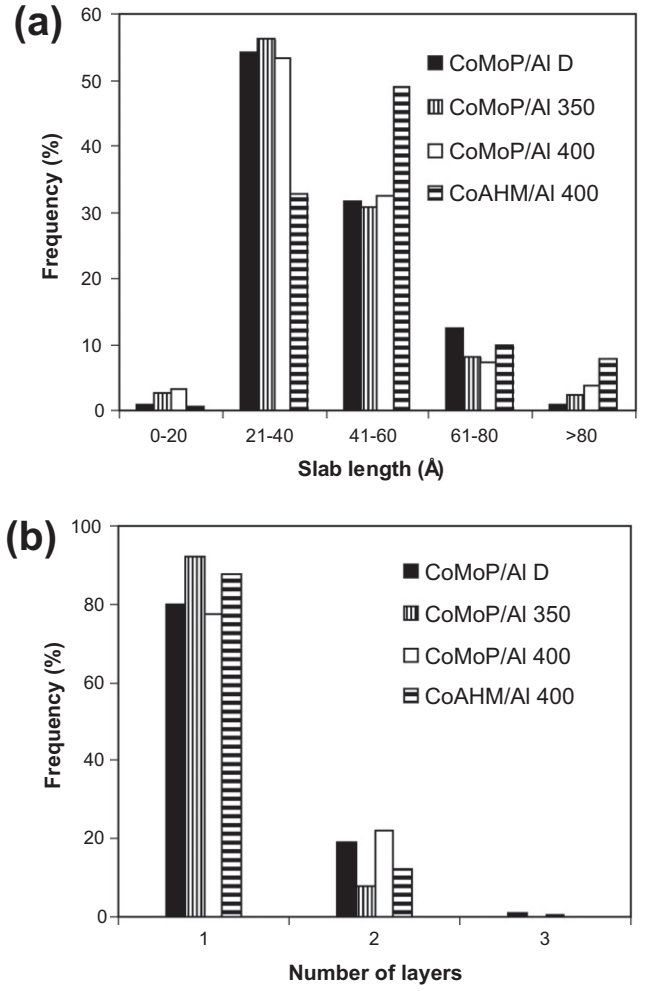

Fig. 7. Distribution of (a) slab length and (b) number of layers of MoS_2 crystallites.

and corners are given in Table 3. The estimation of these latter values was made using the MoS_2 geometric models reported in the study by Kasztelan et al. [37–40].

The results in Table 3 indicate that there is little difference between the catalysts prepared with $Co_{7/2}PMo_{12}O_{40}$, which show better dispersion than the catalyst prepared conventionally using AHM.

Table 3
Average length (L), number of layers (N), and Mo distribution for MoS_2 crystallites.

Catalyst	L (Å)	N	DMo_e	DMo_c	DMo_T
CoMoP/Al D	40	1.21	0.21	0.04	0.25
CoMoP/Al350	40	1.07	0.21	0.04	0.25
CoMoP/Al400	40	1.22	0.2	0.04	0.24
CoAHM/Al400	47	1.12	0.18	0.03	0.21

DMoe = Mo in edge/total Mo atoms; DMoc = Mo in corner/total Mo; DMo_T = Mo in corner + Mo in edge/total Mo atoms.

3.4. Catalytic activity in HDS of 4,6-DMDBT

The conversion of 4,6-DMDBT at 320 °C 1200 psi after 6-h reaction in a batch reactor and the pseudo-first-order rate constants are shown in Table 4. All catalysts prepared with $Co_{7/2}PMo_{12}O_{40}$ are more active than the conventionally prepared CoAHM/Al400, which according to the HRTEM results presents lower dispersion of the sulfide phase (Table 3).

For the catalysts prepared with $Co_{7/2}PMo_{12}O_{40}$, the activity decreases with the calcination temperature according to the order: CoMoP/Al D > CoMoP/Al 350 > CoMoP/Al 400. All CoMoP/Al catalysts are more active than CoHMA/Al400; in fact, the rate constant of the uncalcined catalyst (CoMoP/Al D), which presents the highest activity, is about 2.6 times greater than that of CoAHM/Al 400, prepared conventionally with AHM as Mo precursor.

3.5. Selectivity

The selectivity of the reaction is also changed by the preparation method. The main products obtained in the HDS of 4,6-DMDBT were dimethyldiphenyl (DMDP), produced by the direct desulfurization route (DDS), and methylcyclohexyltoluene (MCHT) and dimethyldicyclohexyl (DMDC), produced by the hydrogenation (HYD) route [41–43].

The results (shown in Table 5) indicate that hydrogenation is the main route of transformation of 4,6-DMDBT and that the reaction selectivity, given by the ratio θ = HYD/DDS = (MCHT + DMDC)/DMDP, changes from 6.2 for the uncalcined catalyst to about 4.0 when the catalyst is calcined. Calcination seems to decrease the hydrogenation route and surprisingly slightly enhances the direct

Table 4
Conversion of 4,6-DMDBT and values of pseudo-first-order reaction rate constants calculated for batch reactor operating at: t = 0–6 h, T = 320 °C, P = 1200 psi.

Catalyst	Conversion (%)	$k_{HDS} \times 10^4$ (s^{-1})	$k_{HDS} \times 10^{24}$ (1/s-atom of Mo)
CoMoP/Al D	91	1.19	1.39
CoMoP/Al 350	87	0.94	1.06
CoMoP/Al 400	85	0.86	1.04
CoAHM/Al 400	62	0.47	0.52

Table 5
Product concentrations from hydrogenation (HYD) and direct desulfurization (DDS) routes at 40% 4,6-DMDBT conversion and selectivity ratio θ = HYD/DDS.

Catalysts	$HYD_{40\%}$ (mol/l) $\times 10^3$	$DDS_{40\%}$ (mol/l) $\times 10^3$	θ
CoMoP/Al D	8.1	1.3	6.2
CoMoP/Al 350	7.6	1.8	4.2
CoMoP/Al 400	7.7	1.7	4.5
CoAHM/Al 400	7.5	1.9	3.9

θ = HYD/DDS = (MCHT + DMDC)/DMDP.

desulfurization route. This does not seem to be related to the architecture of the MoS_2 slabs since the average length and stacking do not show any clear tendency with calcinations. Although the decrease in hydrogenation with the calcination temperature could be explained by the formation of type I CoMoS structures interacting with the support and not well sulfided, the observed slight increase in DDS is not clear yet.

The observed activity decrease for CoMoP catalysts with the calcination temperature can be explained by formation of large MoO_3 particles, which in turn lead to lower dispersion. The results from XRD indicated that for CoMoP/Al 400, some MoO_3 is formed. The results from Raman analysis also support the formation of MoO_3 in CoMoP/Al400. The Raman spectrum of CoMoP/Al 400 displays two not so well-defined Raman bands, one at ≈952 cm^{-1}, which can be assigned to the presence of polymolybdates [22], and another at ≈827 cm^{-1} associated with the formation of MoO_3 crystallites; this band grows more intense as the calcination temperature is increased to 500 °C (not shown). However, the HRTEM observations of the sulfided catalysts indicated almost the same dispersion of the MoS_2 crystallites for all the catalysts prepared with $Co_{7/2}PMo_{12}O_{40}$. So, a different cause for the drop in activity must be found. It is possible that the cause for the observed decrease in activity with calcination temperature be due to a lower promotion of Mo by Co since during calcination at increasing temperatures decomposition of the Keggin structure occurs leading to higher amounts of segregated molybdenum and cobalt oxides, which are not efficiently transformed into the CoMoS-promoted active phase during sulfidation. This possibility will be analyzed below by FTIR-analyzed CO adsorption over the sulfided catalysts since CO can efficiently titrate and differentiate the promoted and unpromoted Mo sites.

CO adsorption is a powerful tool for the characterization of sulfided Mo-based HDS catalysts promoted by Co or Ni. It is possible to obtain information on the coordinatively unsaturated sites (CUS) located in promoted and non-promoted Mo sites. The spectra of adsorbed CO at 1.0 Torr equilibrium are presented in Fig. 8.

All spectra show a band at 2190 cm^{-1} that corresponds to CO adsorbed on Lewis acid sites (Al^{3+}), and other one at 2156 cm^{-1}, assigned to CO interacting with hydroxyl groups (Brønsted sites) [28,29]. At lower wavenumbers, bands corresponding to CO interacting with the sulfide phase are evident. The band at 2110 cm^{-1} is characteristic of CO adsorbed on non-promoted Mo sites, and the band at 2070 cm^{-1} has been assigned to the interaction of CO with promoted CoMoS sites [29,41].

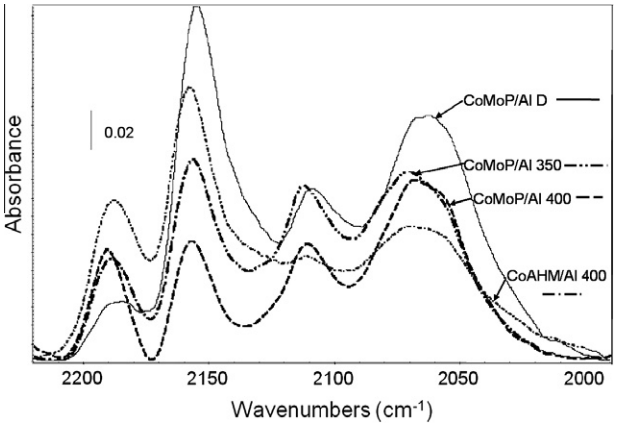

Fig. 8. FTIR spectra of CO adsorbed over sulfided catalysts at 1.0 Torr equilibrium.

The intensity of the band at 2070 cm^{-1}, associated with CoMoS sites, is maximum for CoMoP/Al D and decreases with the calcination temperature; this decrease is even larger for the CoAHM/Al 400.

As for the intensity of the band associated with non-promoted Mo sites (∼2110 cm^{-1}), it is slightly greater for CoMoP/Al 350 than for CoMoP/Al D. It appears that the relative increase in non-promoted Mo sites in CoMoP/Al 350, occurs at the expense of some of the promoted sites. The intensity of this band for CoMoP/Al400 and CoAHM/Al 400, both calcined at 400 °C, is even lower possibly due to an incomplete sulfidation of the Mo phase resulting from the strong interaction with the support induced by the high temperature of calcination. These results suggest that calcination at high temperatures leads to a lower number of promoted and non-promoted sites and is detrimental to catalyst activity.

In the region of CO adsorbed on the support, CoMoP/Al D shows a low intensity in the band associated with Lewis Al^{3+} sites and high intensity of the band of CO interacting with OH groups. This means that the Mo-supported phases are not interacting with the hydroxyl groups on the support, possibly because this catalyst was not calcined, and therefore, the formation of Mo–O–Al bridges, which normally involves the hydroxyl groups and are formed during the calcination step, did not take place. Other possibility is that this catalyst is better sulfided due to a weak interaction of the heteropolyacid salt with the support, and therefore, full sulfidation of the catalyst precursor leads to the recovery of the support hydroxyl groups. The high intensity of the band associated with OH's cannot be the result of poor dispersion of the Mo sulfide phase because the intensity of the bands associated with Mo (promoted and non-promoted), which give an indication of the Mo dispersion, is big for this catalyst compared with the other ones. Moreover, the XRD and HRTEM results also indicate good dispersion of Mo in CoMoP/Al D. The fact that the Al^{3+} sites are depleted in this catalyst indicates that some of the Mo-sulfided species are interacting or located on top of Al Lewis sites. It is interesting that similar results are obtained for the unpromoted catalyst, MoP/Al D, which in dry state presents a hydroxyl band larger than the one associated with Mo sites (Fig. 9).

The ratio of promotion, estimated as the area under the curve of the band associated with promoted sites (2070 cm^{-1}) over non-promoted ones (2110 cm^{-1}), changes from 2.2 for CoMoP/Al D to 1.4 for CoAHM/Al 400, indicating that the use of $Co_{7/2}PMo_{12}O_{40}$ allows higher promotion levels.

To compare the catalysts in a more quantitative way, it is necessary to estimate the intrinsic activity of each Mo site (promoted and non-promoted). The total activity displayed by a catalyst would be the sum of the contributions of the number of each type

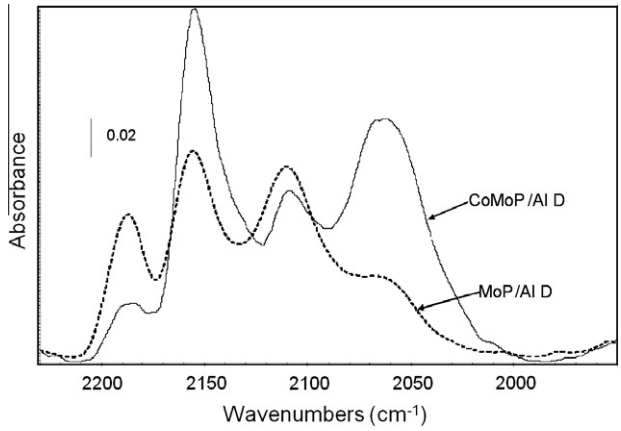

Fig. 9. FTIR spectra of CO adsorbed over dried promoted and non-promoted sulfided catalysts.

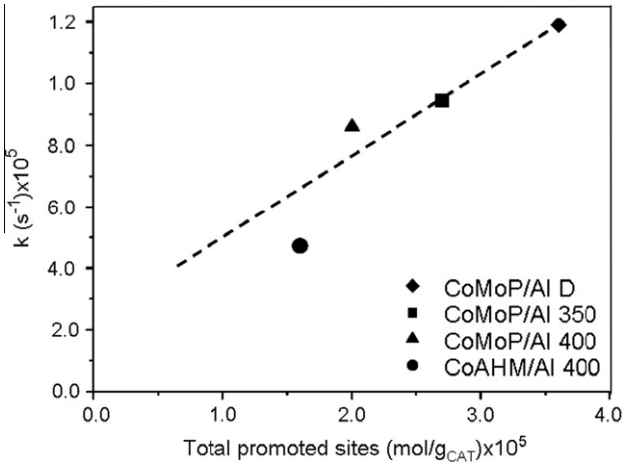

Fig. 10. Variation in rate constant vs concentration of promoted CoMoS sites.

of sites multiplied by its intrinsic activity; this can be expressed mathematically as follows:

$$a_T = N_{Mo}(a_{Mo}) + N_{CoMoS}(a_{CoMoS}) \quad (1)$$

where a_T is the total activity of the catalyst; N_{Mo} is the number of non-promoted Mo sites; a_{Mo} is the intrinsic activity of non-promoted site; N_{CoMoS} is the number of promoted Mo sites; a_{CoMoS} is the intrinsic activity of CoMoS site.

The number of each type of site can be estimated from its corresponding IR band, and the total activity is obtained from the activity test. The intrinsic activity of the unpromoted site can be calculated using the total activity obtained with MoP/Al D or MoP/Al 400 and only the first term of the right-hand side of Eq. (1). The results displayed in Table 6 show that the intrinsic activity of the non-promoted site in the catalyst calcined at 400 °C is slightly lower than that of its non-calcined counterpart, MoP/Al D. This could be due to the fact that part of the Mo in the calcined catalyst is interacting with the support through Mo–O–Al bridges, lowering the activity of the sulfided sites.

To estimate the intrinsic activities of the promoted sites, a set of two equations must be solved. The calculated values of the intrinsic activities of CoMoS sites given in Table 6 were obtained using the intrinsic activities of unpromoted Mo sites estimated earlier. A significant difference is observed between the activity of CoMoS sites in the catalysts prepared with heteropolyacid salt and that of the conventionally prepared catalyst. Moreover, a plot of the concentration of promoted sites versus the activity of the catalysts expressed as the pseudo-first-order rate constant Fig. 10 shows a linear correlation for the catalysts prepared with $Co_{7/2}PMo_{12}O_{40}$ but the conventionally prepared catalyst is outside the general trend. These results can be explained by the existence of promoted sites with different activity, as suggested before [44]. In fact, a close observation of the band at 2070 cm^{-1} reveals the presence of a shoulder at 2055 cm^{-1}, which is more defined for the catalysts calcined at 400 °C. These two bands have been reported before [44]. By combining infrared spectroscopy and periodic DFT calculations, Travert et al. [44] studied the structure and the nature of CO adsorption sites on CoMoS phases. According to their results, the promoted $CoMo/Al_2O_3$ catalyst was characterized by a broad band at 2070 cm^{-1} and a shoulder at ~2055 cm^{-1} that are specific of the promotion. The band at 2070 cm^{-1} was assigned to CO interacting with different structures containing Mo and Co, penta (5c) or tetra (4c) coordinated, such as (i) edge of Mo in Co4c; (ii) edge of Mo in Mo5c; and (iii) edge of S en Co4c. These three sites are named here CoMoS-A sites. The shoulder at 2055 cm^{-1}, named here CoMoS-B, was related to CO interacting with Mo4c in the edge of S.

To estimate the intrinsic activity of these two types of promoted sites, two simultaneous equations with the form of Eq. (2) must be solved using data obtained from two different catalysts, and the intrinsic activity of unpromoted Mo sites estimated earlier.

$$a_T = N_{Mo}(a_{Mo}) + N_{CoMoS-A}(a_{CoMoS-A}) + N_{CoMoS-B}(a_{CoMoS-B}) \quad (2)$$

where a_T is the total activity of the catalyst; N_{Mo} is the number of non-promoted Mo sites; a_{Mo} is the intrinsic activity of non-promoted Mo site; $N_{CoMoS\text{-}A}$ is the number of promoted CoMoS-A sites; $a_{CoMoS\text{-}A}$ is the intrinsic activity of CoMoS-A site; $N_{CoMoS\text{-}B}$ is the number of promoted CoMoS-B sites and $a_{CoMoS\text{-}B}$ is the intrinsic activity of CoMoS-B site.

The calculated number of sites from a deconvolution using a Peak Fit software and intrinsic activities for each type of site are given in Table 7. Indeed, the results show that CoMoS-A and CoMoS-B have different activities and that the activity of CoMoS-B (band at 2055 cm^{-1}) is about 18% more active than CoMoS-A (band at 2070 cm^{-1}). It is also shown that avoiding calcination for the catalyst prepared with $Co_{7/2}PMo_{12}O_{40}$ leads to higher number of promoted CoMoS-B sites, which are the most active. More than 50% of these sites seem to be destroyed by calcination even at 350 °C.

Table 6
Quantification and intrinsic activity of promoted (CoMoS) and non-promoted (Mo) sites from CO adsorption.

Catalysts	Mo sites 2110 cm^{-1} (mol/g_{cat}) × 10^5	CoMoS sites 2070 cm^{-1} (mol/g_{cat}) × 10^5	$a_{MoS2\ site}$ (s^{-1}) × 10^3	$a_{CoMoS\ site}$ (s^{-1}) × 10^2	Total sites (mol/g_{cat}) × 10^5
MoP/Al D	5.5		5.5		5.5
MoP/Al 400	3.2		4.8		3.2
CoMoP/Al D	2.6	3.6		1.3	6.2
CoMoP/Al 350	3.0	2.7		1.2	5.7
CoMoP/Al 400	1.7	2.0		1.9	3.7
CoAHM/Al 400	1.8	1.6		0.9	3.4

Table 7
Quantification and intrinsic activities of promoted CoMoS sites.

Catalysts	Mo sites 2110 cm^{-1} (mol/gcat) $\times 10^6$	CoMoS-A 2070 cm^{-1} (mol/gcat) $\times 10^6$	CoMoS-B 2055 cm^{-1} (mol/gcat) $\times 10^6$	Total HDS activity (a_T) (mol/s-g) $\times 10^7$ From 4,6-DMDBT test	Total HDS activity (a_T) (mol/s-g) $\times 10^7$ Calculated from Eq. (2)	$a_{CoMoS-A}$ 2070 cm^{-1} (s^{-1}) $\times 10^2$	$a_{CoMoS-B}$ 2055 cm^{-1} (s^{-1}) $\times 10^2$
CoMoP/Al D	28	19	20.1	6.2	6.2	1.1	1.3
CoMoP/Al350	31	21	7.8	4.7	4.7	1.1	1.3
CoMoP/Al 400	17	13	9.4	4.6	3.4	1.1	1.3
CoAHM/Al 400	18	11	9.0	2.2	3.1	1.1	1.3

Note: The molar extinction coefficient of the band at 2055 cm^{-1} is considered equal to that of the band at 2070 cm^{-1}.

3.6. Temperature Programmed Sulfidation (TPS)

To analyze whether the use of $Co_{7/2}PMo_{12}O_{40}$ helps the sulfidation process of the catalyst, TPS experiments with CoMoP/Al D, CoMoP/Al 400, and CoAHM/Al 400 were carried out. Fig. 11 shows that in general, there is an initial consumption of H_2S associated with the partial or total sulfidation of Mo^{6+} species, followed by an evolution of H_2S associated with the reduction in sulfided Mo^{6+} to sulfided Mo^{4+} species. The final H_2S uptake corresponds to the complete sulfidation of Mo^{4+}. The presence of more than one H_2S evolution indicates the reduction in Mo^{6+} species with different degree of sulfidation [45].

CoMoP/Al D reaches total sulfidation and shows a very small intermediate H_2S evolution peak, indicating that the further sulfidation of Mo^{4+} occurs faster than for CoMoP/Al 400 and CoAHM/Al 400. In fact, the latter two catalysts do not achieve total sulfidation since the trace does not reach the base line. This means that the interaction of the precursor with the support is stronger for CoMoP/Al 400 and CoHMA/Al 400 than for CoMoP/Al D [45,46]. This could well be the reason for the lower total number of Mo sites (non-promoted + promoted) detected by CO (see Table 6) for the former catalysts. Table 6 also shows that the fraction of promoted sites is higher for CoMoP/Al D, corroborating that higher promotion is obtained without calcining the catalyst prepared with $Co_{7/2}PMo_{12}O_{40}$.

The results obtained here show that the use of $Co_{7/2}PMo_{12}O_{40}$ as catalyst precursor favors a high dispersion of the active MoS_2 phase and a higher number of CoMoS-promoted sites in comparison with a catalyst prepared with AHM and $Co(NO_3)_2$ precursors. CO adsorption proved to be an important tool for the characterization of the sulfided phase, and by this technique, it was possible to show that more than one CoMoS structures with different activities can coexist in the catalyst. Development of future catalysts should consider the optimization of the number of promoted sites with the highest intrinsic activity.

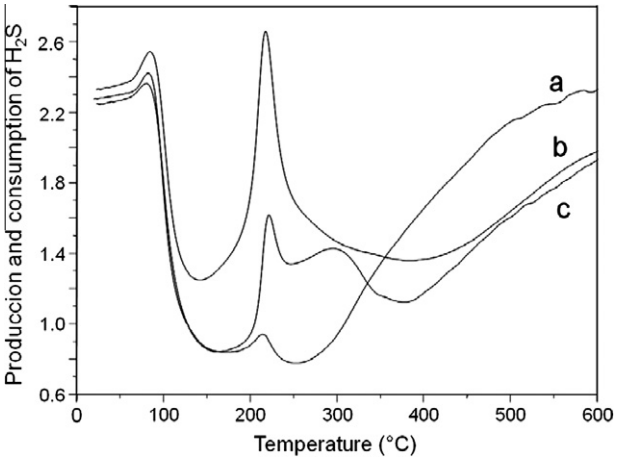

Fig. 11. TPS thermograms of: (a) CoMoP/Al D, (b) CoMoP/Al 400, and (c) CoAHM/Al 400.

4. Conclusions

The activity in the HDS of 4,6-DMDBT of calcined and non-calcined CoMoP/Al_2O_3 catalysts prepared with $Co_{7/2}PMo_{12}O_{40}$ was compared with that of a catalyst prepared conventionally with ammonium heptamolybdate, cobalt nitrate, and phosphoric acid. The extent of promotion for each method of preparation was quantitatively determined by CO adsorption. From these experiments, the intrinsic activity of the different coordinatively unsaturated Mo sites present in the sulfided catalyst was evaluated. The results led us to the following conclusions:

(1) The use of $Co_{7/2}PMo_{12}O_{40}$ as precursor of CoMoP HDS catalysts leads to higher activity than that of a catalyst prepared by coimpregnation of a mixture of ammonium heptamolybdate–cobalt nitrate–phosphoric acid. The increased activity of the former catalyst was related to a higher number of Co-promoted molybdenum sites.
(2) The amount of Co-promoted sites in the catalyst prepared with $Co_{7/2}PMo_{12}O_{40}$ depends on the pretreatment given to the catalyst before its activation (sulfidation). High activity is obtained by avoiding the calcination treatment, and for the calcined catalysts, the activity decreases with the calcination temperature. This is related to the stability of the Keggin structure of $Co_{7/2}PMo_{12}O_{40}$ that is destroyed at calcination temperatures above 350 °C.
(3) Two different types of promoted CoMoS sites with different HDS intrinsic activities seem to coexist in the sulfided catalyst. From the two sites, CoMoS-A (associated with CO-IR band at 2070 cm^{-1}) and CoMoS-B (associated with CO-IR band at 2055 cm^{-1}), the later has higher intrinsic activity.

Acknowledgments

We acknowledge financial support from CONACyT (Project 49479), DGAPA-UNAM (PAPIIT 102709) and financial support from the National Council for Science and Technology of Mexico (CONACYT) (PhD Scholarship to Adolfo Romero Galarza). JR acknowledges sabbatical grant from DGAPA-UNAM. We thank the HRTEM work of Ivan Puente and C. Salcedo for the XRD work. ARG is grateful to P. Castillo for helpful discussions during CO adsorption experiments.

References

[1] B.C. Gates, H. Topsøe, Polyhedron 16 (1997) 3213.
[2] P.G. Moses, B. Hinnemann, H. Topsøe, J.K. Nørskov, J. Catal. 248 (2007) 188.

[3] J.A.R. van Veen, P.A.J.M. Hendricks, R.R. Andrea, E.J.G.M. Romers, A.E. Wilson, J. Phys. Chem. 94 (1990) 5282.
[4] W.C. Cheng, N.P. Luthra, J. Catal. 109 (1988) 163.
[5] P. Atanasova, J. Uchytil, M. Kraus, T. Halachev, Appl. Catal. 65 (1990) 53.
[6] P. Atanasova, T. Halachev, J. Uchytil, M. Kraus, Appl. Catal. 38 (1988) 235.
[7] M. Daage, R.R. Chianelli, J. Catal. 149 (1994) 414.
[8] H. Topsøe, Appl. Catal. A. 322 (2007) 3.
[9] J.V. Lauritsen, J. Kibsgaard, G.H. Olesen, P.G. Moses, B. Hinnemann, S. Helveg, J.K. Nørskov, B.S. Clausen, H. Topsøe, E. Lægsgaard, F. Besenbacher, J. Catal. 249 (2007) 220.
[10] M. Brorson, A. Carlsson, H. Topsøe, Catal. Today 123 (2007) 31.
[11] J.V. Lauritsen, M.V. Bollinger, E. Lægsgaard, K.W. Jacobsen, J.K. Nørskov, B.S. Clausen, H. Topsøe, F. Besenbacher, J. Catal. 221 (2004) 510.
[12] J.V. Lauritsen, M. Nyberg, J.K. Nørskov, B.S. Clausen, H. Topsøe, E. Lægsgaard, F. Besenbacher, J. Catal. 224 (2004) 94.
[13] J.V. Lauritsen, S. Helveg, E. Lægsgaard, Stensgaard, B.S. Clausen, H. Topsøe, F. Besenbacher, J. Catal. 197 (2001) 1.
[14] F. Besenbacher, M. Brorson, B.S. Clausen, S. Helveg, B. Hinnemann, J. Kibsgaard, J.V. Lauritsen, P.G. Moses, J.K. Nørskov, H. Topsøe, Catal. Today 130 (2008) 86.
[15] G. Berhault, M. Perez De la Rosa, A. Mehta, M.J. Yacaman, R.R. Chianelli, Appl. Catal. A 345 (2008) 80.
[16] H. Topsøe, B. Clausen, Appl. Catal. 25 (1986) 273.
[17] H. Topsoe, B.S. Clausen, F.E. Massot, J.R. Anderson, M. Boudart, Catalysis, Science and Technology, vol. 11, Springer, Berlin, 1996.
[18] A. Grivobal, P. Blanchard, L. Gengembre, E. Payen, M. Fournier, J.L. Dubois, J.R. Bernard, J. Catal. 188 (1999) 102.
[19] B. Pawelec, S. Damyanova, R. Mariscal, J.L.G. Fierro, I. Sobrados, J. Sanz, L. Petrov, J. Catal. 223 (2004) 86.
[20] M. Boudart, J.S. Arrieta, R. Dalla Betta, J. Am. Chem. Soc. 105 (1983) 6501.
[21] A. Grivobal, P. Blanchard, E. Payen, M. Fournier, J.L. Dubois, Stud. Surf. Sci. Catal. 106 (1997) 181.
[22] P. Blanchard, C. Lamonier, A. Griboval, E. Payen, Appl. Catal. A 322 (2007) 33.
[23] A. Griboval, P. Blanchard, L. Gengembre, E. Payen, M. Fournier, J.L. Dubois, J.R. Bernard, J. Catal. 188 (1999) 102.
[24] A. Griboval, P. Blanchard, E. Payen, M. Fournier, J.L. Dubois, J.R. Bernard, Appl. Catal. A 217 (2001) 173.
[25] S. Damyanova, J.L.G. Fierro, Appl. Catal. A 144 (1996) 59.
[26] L. Lizama, T. Klimova, Appl. Catal. B 82 (2008) 139.
[27] C. Rocchiccioli-Detcheff, M. Amirouche, M. Fournier, J. Catal. 138 (1992) 445.
[28] F. Maugé, J.C. Lavalley, J. Catal. 137 (1992) 69.
[29] C. Dujardin, M.A. Lelias, J. van Gestel, A. Travert, J.C. Duchet, F. Mauge, Appl. Catal. A 322 (2007) 46.
[30] C. Rocchicicioli-Deltcheff, M. Fournier, R. Franck, R. Thouvenot, Inorg. Chem. 22 (1983) 207.
[31] J.-M. Tatibouët, C. Montalescot, K. Brückman, J. Haber, M. Che, J. Catal. 169 (1997) 22.
[32] G. Mestl, T. Ilkenhans, D. Spielbauer, M. Dieterle, O. Timpe, J. Kröhnert, F. Jentoft, H. Knözinger, R. Schlögl, Appl. Catal. A 210 (2001) 13.
[33] C. Lamonier, C. Martin, J. Mazurelle, V. Harle, D. Guillaume, E. Payen, Appl. Catal. B 70 (2007) 548.
[34] R. Iwamoto, J. Grimblot, Adv. Catal. 44 (1999) 417.
[35] J.A.R. Van Veen, P.A.J.M. Hendriks, R.R. Andrea, E.J.G.M. Romers, A.E. Wilson, J. Phys. Chem. 94 (1990) 5282.
[36] H. Kraus, R. Prins, J. Catal. 164 (1996) 251.
[37] S. Kasztelan, H. Toulhoat, J. Grimblot, J.P. Bonnelle, Appl. Catal. 13 (1984) 127.
[38] E. Payen, R. Hubaut, S. Kasztelan, O. Poulet, J. Grimblot, J. Catal. 147 (1994) 123.
[39] E.J.M. Hensen, P.J. Kooyman, Y. Van der Meer, A.M. van der Kraan, V.H.J. de Beer, J.A.R. van Veen, R.A. van Santen, J. Catal. 199 (2001) 224.
[40] H. Topsøe, B.S. Clausen, Catal. Rev. – Sci. Eng. 26 (1984) 395.
[41] D.D. Whitehurst, T. Isoda, I. Mochida, Adv. Catal. 42 (1998) 345.
[42] M. Egorova, R. Prins, J. Catal. 224 (2004) 278.
[43] F. Sánchez, J. Ramírez, R. Cuevas, A. Gutierrez, C. Fernández, Ind. Eng. Chem. Res. 48 (2009) 1178.
[44] A. Travert, C. Dujardin, F. Mauge, E. Veilly, S. Cristol, J.F. Paul, E. Payen, J. Phys. Chem. B 110 (2006) 1261.
[45] P. Arnoldy, J.A.M. van den Heijkant, G.D. de Bok, J.A. Moulijn, J. Catal. 92 (1985) 35.
[46] B. Scheffer, P. Arnoldy, J.A. Moulijn, J. Catal. 112 (1988) 516.